

Heavy-Fermion Quasiparticles in UPT₃

L. Taillefer and G. G. Lonzarich

Cavendish Laboratory, Cambridge CB30HE, United Kingdom

(Received 21 October 1987)

The quasiparticle band structure of the heavy-fermion superconductor UPT₃ has been investigated by means of angle-resolved measurements of the de Haas-van Alphen effect. Most of the results are consistent with a model of 5 quasiparticle bands at the Fermi level corresponding to Fermi surfaces similar to those calculated by band theory. However, as inferred from the extremely high cyclotron masses, the quasiparticle bands are much flatter than the calculated ones. The nature of the observed quasiparticles and their relationship to thermodynamic properties are briefly considered.

PACS numbers: 71.28.+d, 71.25.Hc, 71.25.Jd, 71.25.Pi

The intermetallic compound UPT₃ exhibits thermodynamic properties with remarkable temperature dependences at low temperatures, and below 0.5 K it condenses into an unusual superconducting state which remains one of the outstanding enigmas in condensed-matter physics.¹ In attempts to explain this low-temperature behavior, it has been conventional to invoke a picture of strongly renormalized quasiparticles, i.e., fermions with effective masses orders of magnitude larger than the free-electron mass and having important residual interactions which lead to bound pair formation in the ground state.

To help provide a firm basis for such a quasiparticle description, we have carried out an investigation of the de Haas-van Alphen (dHvA) effect in UPT₃ which yields direct evidence for the existence of heavy fermions and specific information on the Fermi surface and cyclotron masses which characterize them. The initial observation of the dHvA effect in UPT₃ was communicated in a previous paper² and here we present the results of a detailed angle-resolved study, which yield unambiguous information about the quasiparticle band structure near the Fermi level.

The information which may be inferred from the quantum oscillatory (dHvA) magnetization \tilde{M} has been summarized recently² and here we shall reiterate the main points only. First, from the frequency $F(\hat{H})$ of each of the several oscillatory components in $\tilde{M}(\hat{H})$, measured as a function of the orientation of the magnetic field \hat{H} , we infer the cross-sectional area A of the corresponding extremal orbit on the Fermi surface via the Onsager relation $A(\hat{H}) = (2\pi e/\hbar c)F(\hat{H})$, and hence over all we obtain the dimension and topology of the Fermi surface. Second, from the temperature dependence of the amplitude of each oscillatory component, which was found to follow closely the behavior expected for a normal Fermi liquid, we obtain directly the cyclotron effective mass

$$m^*(\hat{H}) = \frac{\hbar^2}{2\pi} \left(\frac{\partial A(\hat{H})}{\partial \epsilon} \right)_{\epsilon_F} = \frac{\hbar}{2\pi} \oint \frac{dk}{v_{\mathbf{k}}},$$

where $v_{\mathbf{k}} = |\hat{H} \times \nabla_{\mathbf{k}} \epsilon|/\hbar$ is the appropriate quasiparticle velocity at the Fermi energy ϵ_F and the integral is over the perimeter of A (on the cyclotron orbit). We may think of m^* as $\hbar k_0/v_0$, where $k_0 = (A/\pi)^{1/2}$ is an average radius and $1/v_0$ is an average of the inverse of the quasiparticle velocity for the cyclotron orbit. Here we shall focus attention on these two properties, namely $A(\hat{H})$ and $m^*(\hat{H})$, which characterize the real part of the quasiparticle energy bands near the Fermi energy ϵ_F ,

TABLE I. Measured dHvA frequencies (F) and cyclotron masses (m^*) for a magnetic field applied along the a and b axes of the hexagonal crystal structure (parallel to the ΓK and ΓM directions in the reciprocal lattice, respectively). The values quoted refer to a field strength of 100 kG. Note that the estimate of a cyclotron mass for the λ branch is only approximate. Also given are the identifications of the measured dHvA branches with extremal orbits on the Fermi-surface model of Fig. 2. dHvA branches are labeled as in Fig. 1, and Fermi-surface orbits are labeled according to their center in the Brillouin zone (e.g., Γ) and their Fermi-surface sheet number (e.g., 1). The calculated a axis results of Wang *et al.* (Ref. 3) for F and m^* are compared with the experimental values.

Branch:FS orbit	F (MG)		m^*/m_e	
	Expt.	Calc.	Expt.	Calc.
a axis (ΓK)				
$\alpha:ML4$	5.4(3)	10.4	25(3)	2.2
$\beta:L4$	6.0(4)	5.2	...	1.0
$\gamma:\Gamma1$	7.3(3)	8.2	40(7)	2.0
$\delta:A5$	14.0(3)	9.1	50(8)	1.9
$\epsilon:\Gamma2$	21.0(3)	24.0	60(8)	4.6
$\omega:\Gamma3$	58.5(5)	52.8	90(15)	5.3
b axis (ΓM)				
$\alpha:ML4$	4.1(2)		15(5)	
$\delta:A5$	12.3(2)		30(3)	
$\theta:A4,5$	15.5(2)		35(7)	
$\phi:A4,5$	18.7(3)		40(8)	
$\psi:A4,5$	21.9(4)		...	
$\lambda:A4$	25.1(5)		(50)	

i.e., their relative positions and their slopes at ϵ_F .

The dHvA magnetization was measured by a low-frequency and low-noise field-modulation technique with a 14.5-T superconducting magnet and a 17-mK dilution refrigerator. The orientation of the sample was varied *in situ*. Measurements for field orientations in the basal plane from a to b in the hexagonal (SnNi_3) crystal structure and from a to c and b to c were performed on two single-crystal disks of comparable size and purity. The first was cut with its normal along the c axis, and the second with its normal along the a axis. Details on crystal preparation and on the experimental procedure may be found in previous papers.²

Our main experimental results are presented in Table I and Fig. 1. Table I is a summary of the measured dHvA frequencies and associated cyclotron masses for directions of the magnetic field along the a and b axes. A total of ten different fundamental frequency components (or branches) are well resolved, with frequencies ranging from 4.1 to 58.5 MG. The highest frequency corresponds to an orbit area roughly as large as one would expect from the size of the Brillouin zone and indeed comparable to the largest extremal areas predicted by band-structure calculations (see below).

The most remarkable of our observations is the extreme magnitude of the cyclotron masses. A detailed study of the temperature dependence of the dHvA amplitudes (performed as described previously²) yields the

cyclotron-mass values listed in Table I. They range from $25m_e$ to $90m_e$ for frequencies along the a axis and from $15m_e$ to approximately $50m_e$ along the b axis. Although these are large variations in m^* , they scale roughly with frequency, which is a common finding, and they *all* represent enormous values compared with masses in simple metals. The ω branch has the highest cyclotron mass observed so far in any metal.

The orientation dependence of the dHvA frequencies is shown in Fig. 1 for field directions in the planes spanned by the crystallographic axes a - c , a - b (the basal plane), and b - c . Only the fundamental components are displayed, although second harmonics of the α and δ branches were also observed. No dHvA oscillations were observed for a field direction in the vicinity of the hexagonal c axis. To some extent, this is a consequence of the general tendency for all frequencies to increase rapidly as the field orientation approaches the c axis (from either the a or the b axis). Indeed, a frequency increasing rapidly with angle implies a large curvature of the Fermi surface and usually an increasing cyclotron mass. Both of these factors conspire to reduce the amplitude of the dHvA oscillation which may eventually fall below the level of detection. Nevertheless, this remains an unusual result.

It is of interest to note that fine structure was observed on the δ branch and on the ω branch. In both cases the multiple fine splitting of the dominant frequency (the one displayed in Fig. 1), resolved into several close frequencies at the highest fields, may be due to a field-induced exchange splitting combined with magnetic breakdown. This structure is currently under investigation.

It is informative to consider our dHvA results in relation to conventional energy-band models. Several calculations based on the local-density approximation to the exchange-correlation potential, with the assumptions that the uranium f electrons are itinerant, have been presented and they all predict similar band structures.³⁻⁵ Nevertheless, slight differences in the precise positions of the five bands found to cross the Fermi level lead to a few significant topological differences in the Fermi surface predicted by the various models. Figure 2(a) shows a Γ ALM section through the Fermi surface obtained by Wang *et al.*³ using the linear muffin-tin orbital method with so-called combined correction terms. Their calculations based on the linearized augmented plane-wave (LAPW) method and the earlier calculations of Oguchi and Freeman (see Ref. 4) and of Albers, Boring, and Christensen⁵ also lead to essentially the same Fermi surface, provided adjustments are made in the positions of two bands with respect to the Fermi level by an amount of order 5 mRy (or less), i.e., within computational accuracy. In this way, for example, the two nested toroidal surfaces centered on point A in the original Fermi surface of Oguchi and Freeman become disks as in Fig. 2.

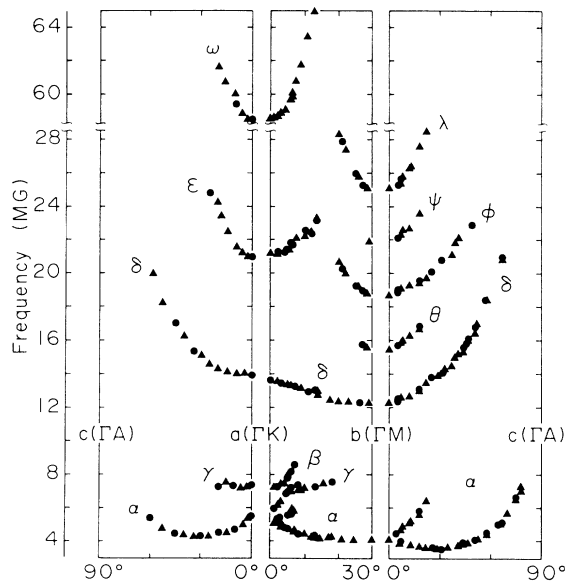


FIG. 1. Variation of the fundamental dHvA frequencies with orientation of the magnetic field in the crystallographic planes a - b , a - c , and b - c . The frequency branches θ , ϕ , and ψ are thought to arise from magnetic breakdown between orbits directly responsible for the δ and λ branches. Harmonic branches of α and δ and fine structure of the δ and ω branches are not displayed.

Most features of the elaborate set of dHvA branches measured as a function of angle find a plausible explanation within this model. For example, the large number of branches near the a axis is matched by an equal number of extremal orbits in planes normal to that axis. Best understood is the behavior of the δ branch which is observed over a wide angular range. Its slow variation in the basal plane and rapid increase towards the c axis unambiguously identifies the existence of a disk-shaped surface like sheet $A5$. The pair of symmetry-related a branches are also well characterized and they exhibit the pattern to be expected from orbits around the upper and lower sections of the L -centered toroidal part of sur-

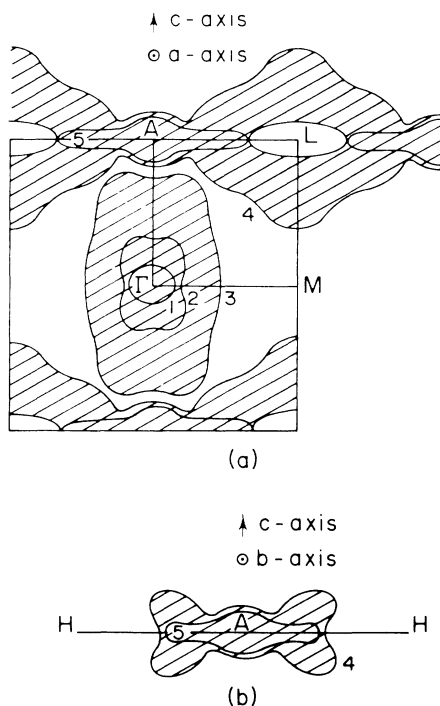


FIG. 2. (a) Γ ALM section through the Fermi surface of UPt₃ derived from conventional band-structure calculations (Ref. 3). The Fermi surface consists of five sheets: two closed electron surfaces centered on Γ (1 and 2), one closed hole disk centered on A (5), one chainlike hole surface extending along AL (4), and one large electron surface centered on Γ (3) which extends along ΓK (a axis) to reach the edge of the Brillouin zone at K . An identification of the observed dHvA frequency branches with extremal orbits on this Fermi surface is given in Table I. (b) Γ AHK section (normal to b axis) through sheets 4 and 5 of the Fermi surface. Magnetic breakdown between these two hole surfaces (for a sufficiently strong magnetic field, along the b axis) occurring at any two of the four nearly degenerate points will give rise to three orbits intermediate in area between the "pure" orbits $A4$ and $A5$. This mechanism provides a natural explanation for the five equally spaced frequency branches δ , θ , ϕ , ψ , and λ observed along the b axis. (The Fermi-surface label convention is that of Refs. 2 and 4 and differs from that of Refs. 3 and 6.)

face 4.

Also accounted for by the Fermi-surface model is the complex feature involving the five branches δ , θ , ϕ , ψ , and λ . Their frequencies on the b axis are separated from each other by precisely the same amount, a strong indication that the three intermediate components θ , ϕ , and ψ arise from magnetic breakdown between the quasiparticle orbits directly associated with the δ and λ branches. A Γ AHK section through sheets 4 and 5 is shown in Fig. 2(b) to illustrate how these two sheets of the Fermi-surface model are seen to provide a natural explanation of those five upper branches.

In Table I, an identification is given of all dHvA branches of Fig. 1 with extremal orbits on the Fermi surface under consideration. At this stage, our identification is based on the salient topological features mentioned above and remains qualitative. Perhaps more importantly, it overlooks certain (potentially significant) details, such as the absence in the data of a low-frequency isotropic branch extending over all angles, as would be expected from a small spherical pocket such as the Γ -centered sheet 1 in Fig. 2(a). It is therefore not entirely conclusive. A more stringent test of the Fermi-surface model requires a quantitative analysis of *all* predicted branches as functions of angle and a detailed comparison with the complete dHvA data. This analysis is currently under way.

On the basis of the present identification, we list in Table I, next to our measured frequencies and masses, the corresponding results calculated by Wang *et al.* for the a axis. It is seen that the calculated extremal areas agree well with the measured frequencies (in fact, these can be made to agree exactly by our shifting the bands at the Fermi level by less than 3 mRy).

The conclusion, supported by the calculations of the orientation dependence of the extremal Fermi-surface areas by Norman *et al.*,⁶ is that where comparison can be made the experimental and calculated Fermi surfaces of UPt₃ are in good agreement. The agreement is similar to, or even better than, that previously reported in other metals with very strong magnetic susceptibilities at low temperatures.

On the other hand, as seen in Table I, the measured and calculated cyclotron masses are far apart. The mass-renormalization factor, i.e., the ratio of measured to (conventional) band-calculated cyclotron masses, is the highest so far reported and lies in the approximate range of 10 to 25. The relative uniformity of this factor among the different bands crossing the Fermi level is characteristic of the behavior which we have observed in other metals with strong mass renormalization.⁷ We note that the quasiparticle band model under consideration accounts roughly for the observed linear heat capacity in the sense that all sheets of the calculated Fermi surface are observed and the average mass enhancement factor is comparable to the ratio of the measured to the

calculated heat capacities. Hence, it appears that the low-temperature heat capacity, and by implication other low-temperature properties, may be described in this material in terms of well-defined fermion quasiparticles in the usual sense. This remains true despite the fact that the Migdal-Luttinger discontinuity in the bare electron occupation numbers at the Fermi level is extremely small, in contrast to conventional metals, that is of the order of 5% (the inverse renormalization factor).

Although the existence of heavy fermions in UPt_3 , and many of their properties, have been established, the precise physical nature of these quasiparticles remains poorly understood. In a number of transition metals in which the mass-renormalization factor is also large (i.e., up to 5 and 6), a close correspondence has been demonstrated between the relaxation rate of low-energy magnetic fluctuations and the low-temperature entropy or heat capacity.⁸ This correspondence suggests that at least in these materials the quasiparticles may be associated with the spin degrees of freedom, i.e., may be regarded as renormalized by spin fluctuations. A similar description may be appropriate for UPt_3 , and several applications of the above approach proposed for the transition metals have recently been reported for UPt_3 and other actinide and rare-earth heavy-electron systems.^{9,10} However, in UPt_3 , in contrast to the transition metals so far investigated,¹¹ the magnetic fluctuation spectra, as well as the particle density fluctuation spectra, at very low energies are not understood in detail and remain subjects of controversy.¹ Hence, a convincing description of the precise physical nature of the quasiparticles in UPt_3 remains to be worked out.

We wish to thank R. Newbury for his invaluable help

in the early phases of this study and we are indebted to R. Hall, from the Chemistry Division, Atomic Energy Research Establishment, Harwell, for providing the high-quality uranium which was used in the preparation of our samples. This work may not have been started without the initial stimulus and support of J. L. Smith, Z. Fisk, and P. Coleman whose contributions are most gratefully acknowledged.

¹For recent work and references to the earlier literature, see *Theoretical and Experimental Aspects of Valence Fluctuations*, edited by L. C. Gupta and S. K. Malik (Plenum, New York, 1987), and Proceedings of the Eighteenth Yamada Conference on Superconductivity in Highly Correlated Fermion Systems, Sendai, Japan, 1987 (to be published).

²L. Taillefer, R. Newbury, G. G. Lonzarich, Z. Fisk, and J. L. Smith, *J. Magn. Magn. Mater.* **63 & 64**, 372 (1987).

³C. S. Wang, M. R. Norman, R. C. Albers, A. M. Boring, W. E. Pickett, H. Krakauer, and N. E. Christensen, *Phys. Rev. B* **35**, 7260 (1987).

⁴T. Oguchi, A. J. Freeman, and G. W. Crabtree, *J. Magn. Magn. Mater.* **63 & 64**, 645 (1987).

⁵R. C. Albers, A. M. Boring, and N. E. Christensen, *Phys. Rev. B* **33**, 8116 (1986).

⁶M. R. Norman, R. C. Albers, A. M. Boring, and N. E. Christensen, *Solid State Commun.* (to be published).

⁷See, e.g., M. Wulff, G. G. Lonzarich, H. L. Skriver, and D. Fort, to be published, and references cited therein.

⁸G. G. Lonzarich, *J. Magn. Magn. Mater.* **54-57**, 612 (1986).

⁹M. R. Norman, *Phys. Rev. Lett.* **59**, 232 (1987).

¹⁰R. Kanno and T. Moriya, to be published.

¹¹N. R. Bernhoeft, S. M. Hayden, G. G. Lonzarich, and D. McK. Paul, to be published.